CCS Chemistry

RESEARCH ARTICLE

Received: Feb. 1, 2021 | Accepted: Apr. 29, 2021

Finely Tuning the Lower Critical Solution Temperature of Ionogels by Regulating the Polarity of Polymer Networks and Ionic Liquids

Lie Chen[1,2], Cong Zhao[1], Xiaozheng Duan[3]*, Jiajia Zhou[1,4]* & Mingjie Liu[1,4]*

[1]*Key Laboratory of Bio-Inspired Smart Interfacial Science and Technology of Ministry of Education, School of Chemistry, Beihang University, Beijing 100191,* [2]*School of Physics, Beihang University, Beijing 100191,* [3]*State Key Laboratory of Polymer Physics and Chemistry, Changchun Institute of Applied Chemistry, Chinese Academy of Sciences, Changchun 130022,* [4]*International Research Institute for Multidisciplinary Science, Beihang University, Beijing 100191*

**Corresponding authors: xzduan@ciac.ac.cn; jjzhou@buaa.edu.cn; liumj@buaa.edu.cn*

Cite this: *CCS Chem.* **2021**, *3*, 1659–1669

Nonvolatile ionogels have recently emerged as promising soft electrolyte materials due to their high ionic conductivity and good durability. However, the compatibility between polymer networks and ionic liquids (ILs), which show significant influence on the physicochemical properties of the ionogels, has been rarely studied. Herein, we elucidate a lower critical solution temperature (LCST)-type phase behavior of ionogels composed of polyacrylates and hydrophobic 1-alkyl-3-methylimidazolium bis{(trifluoromethyl)sulfonyl}amide ILs. We systematically study the structural effects of ILs and monomers on the LCST of ionogels. Our work illustrates that the LCST of ionogels is primarily determined by the polarity of polymer side chains and the alkyl chain on cations of ILs. The oriented solvation between polymers and ILs caused by hydrogen-bonding effects and van der Waals interactions may serve as the driving force for the LCST phase behavior in our system. Furthermore, by varying the mixing ratio of two structurally similar ILs in their blends, the LCST of ionogels can be tuned to exhibit a linear variation within a wide temperature range (from subzero to over 200 °C). Finally, thermoresponsive ionogels with desired patterns are prepared using photomasks. These nonvolatile ionogels with tunable LCST enriched the functionality of state-of-the-art ionogels, which provides insight into the design and fabrication of smart and flexible electronic/optical devices.

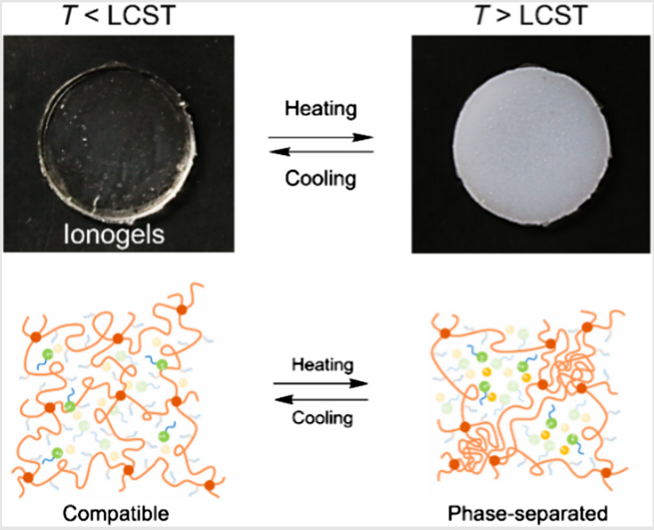

Keywords: ionic liquids, ionogels, LCST, polyacrylates, thermoresponsive, smart window

DOI: 10.31635/ccschem.021.202100855

Introduction

Ionic liquids (ILs) are room temperature molten salts that have drawn great attention due to their appealing properties such as nonvolatility, tunable polarity, wide liquid temperature ranges, and strong solvation ability.[1,2] Due to these well-known properties, particularly the wide electrochemical window and good ionic conductivity, combined with the thermal and chemical stability, ILs have been extensively applied as an ideal electrolyte with good electrochemical performance.[3] Ionogels are composed of three-dimensional (3D) polymer networks and ILs are promising systems, as they can be shaped like solids while simultaneously maintaining the macroscopic properties of ILs.[4,5] Recently, the development of ionogels has offered great potential for electrical, optical, and biomedical applications, such as energy storage and conversion devices,[6–8] transistors,[9–11] actuators,[12,13] and drug delivery and luminescent materials.[14,15]

Ionogels can be classified into three categories according to the nature of the solid-like 3D network, which are organic, inorganic, and organic–inorganic hybrid, respectively. Organic ionogels can be fabricated using low molecular weight gelators or dissolving polymers in ILs directly.[16] The well-known “bucky” gels and silica-based ionogels are typical inorganic ionogels.[17,18] Organic–inorganic hybrid refers to polymeric ionogels reinforced with inorganic fillers.[19] As a facile strategy to prepare ionogel matrices with desired mechanical resistance, the organic 3D network formed by cross-linked polymers is generally adopted and extensively studied. Further, polymeric ionogels may be separated into physical and chemical gels. For physically cross-linked ionogels, the existence of specific functional groups is a prerequisite. For example, in 1-ethyl-3-methylimidazolium bis(trifluoro-methylsulfonyl)imide/poly(vinylidene fluoride-co-hexa-fluoropropylene) ([EMIM][TFSI]/PVDF-HFP) ionogels systems, the PVDF crystallites work as physical cross-linking sites, which provide the mechanical strength to the ionogel.[20] In contrast, chemical cross-linking is a ubiquitous strategy, as ionogels can be directly fabricated by polymerizing target monomers in ILs.

Generally, the properties of ionogels are expected to be derived from both from the ILs and the components forming the 3D network. In reality, the intrinsic character of ionogels relies on the intimate combination of ILs and 3D networks. Recent studies indicate that the nanometer scale assembly may affect the properties of ionogels. For example, in some polymeric ionogels, only one glass transition (lower than the T_g of neat ILs and higher than the T_g of pure polymer) was observed, suggesting a compatible system of ionogels.[21] Consequently, the miscibility between ILs and polymer network directly determines the properties of organic ionogels.

It is worth mentioning that the mutual miscibility between ILs and polymer is not invariable. In certain systems, the solubility of the polymer in ILs can respond to an external stimulus, such as light illumination, heat, and certain chemicals.[22–25] Similar to poly(*N*-isopropylacrylamide) (PNIPAm) that exhibits lower critical solution temperature (LCST) or upper critical solution temperature (UCST) phase behavior in aqueous solutions, polymer/ILs systems exhibit more diverse and sophisticated LCST and UCST phase behavior.[26] For instance, Poly(benzyl methacrylate)/1-alkyl-3-methylimidazolium bis(trifluoromethanesulfone)imide (PBzMA/[C_nMIM][NTf_2]),[27] Poly(n-butyl methacrylate) (PnBMA)/[C_nMIM][NTf_2],[28,29] Polyethylene oxide (PEO)/[C_nMIM]Tetrafluoroborate [BF_4], and polyethers/[C_nMIM][NTf_2] are reported for their typical nature of LCST phase behaviors.[30–32] PNIPAm/[C_nMIM][NTf_2] is a system that possesses UCST phase behavior.[33] However, most relative studies have mainly focused on polymer/ILs solution systems, while the LCST or UCST phase behavior of the ionogel states are rarely investigated. Herein, to fundamentally explore these important thermodynamic phenomena and expand the functionality of the ionogels, polyacrylates/[C_nMIM][NTf_2] ionogels with tunable LCST phase behavior are designed and fabricated based on our previous study.[34]

To understand this phase behavior from a deeper perspective, we systematically investigated the structural effects of ILs and monomers on the LCST phase transition of ionogels. The mechanism of LCST phase behavior is analyzed, and the prerequisites for the LCST phase behavior of the ionogels are proposed. Meanwhile, how hydrogen bonds between polymer and ILs influence the LCST of ionogels are studied. By varying the mixing ratio of two structurally similar ILs in their blends, the LCST of ionogels can be tuned within a wide temperature range. Resemble the effect of molecular weight on LCST in polymer/ILs systems, the LCST of ionogels decreased as increasing the polymerization degree of the monomers. Taking advantage of this property, thermoresponsive ionogels with desired patterns are prepared using a photomask. These nonvolatile ionogels with high optical transparency, tunable LCST, good durability, and wide temperature range mechanical stability show promising applications in fields related to flexible sensors and “smart” optical devices.

Experimental Methods

Preparation of ionogels

Butyl acrylate (monomer), ethyleneglycol dimethacrylate (EGDMA, cross-linker), and diethoxyacetophenone (DEOP, photoinitiator) were dissolved in ILs, and then the mixture was stirred for 10 min until a fully transparent solution was obtained. The polymerization was initiated by UV irradiation, and the solution was cured under UV light (365 nm, 800 mW/cm^2) for 10 min.

Mechanical characterization

The mechanical characterization of ionogels was realized using a tensile machine (SUNS, UMT4103, Shenzhen, China). The sample was cut into a dumbbell shape, and both ends of the dumbbell-shaped sample were connected to the clamps with a fixed lower clamp. The upper clamp was pulled by the load cell at a constant velocity of 20 mm/min at room temperature, by which the stress–strain curve was recorded and the experimental data were further analyzed. The tensile strength was obtained from the failure point. We determined the modulus of ionogels by the average slope over 0–10% of strain ratio detected from the stress–strain curve.

LCST characterization of ionogels

The LCST of ionogels was determined by optical transmittance measurements using dynamic light scattering (Litesizer™ 500; Anton Paar, Graz, Austria). A transmittance of 100% indicates ionogel homogeneity, and a decrease in transmittance suggests that the ionogel undergoes LCST phase separation. We define the LCST as the temperatures at which the transmittance drops to 80% (Supporting Information Figure S4).

Thermal analysis

Thermal analysis was conducted using a thermogravimetric analyzer (TGA) (Q500; TA Instruments, New Castle, DE) and a differential scanning calorimeter (DSC) (Q2000; TA Instruments) at a heating rate of 10 °C/min.

Results and Discussion

Preparation and the LCST phase behavior of ionogels

The ionogels were fabricated by in situ photoinduced polymerization (Supporting Information Figure S1) of acrylates monomers in ILs using EGDMA and DEOP as cross-linker and photoinitiator (Figures 1b and 1c), respectively. Polyacrylates are typically used to prepare functional elastomer matrices due to their good

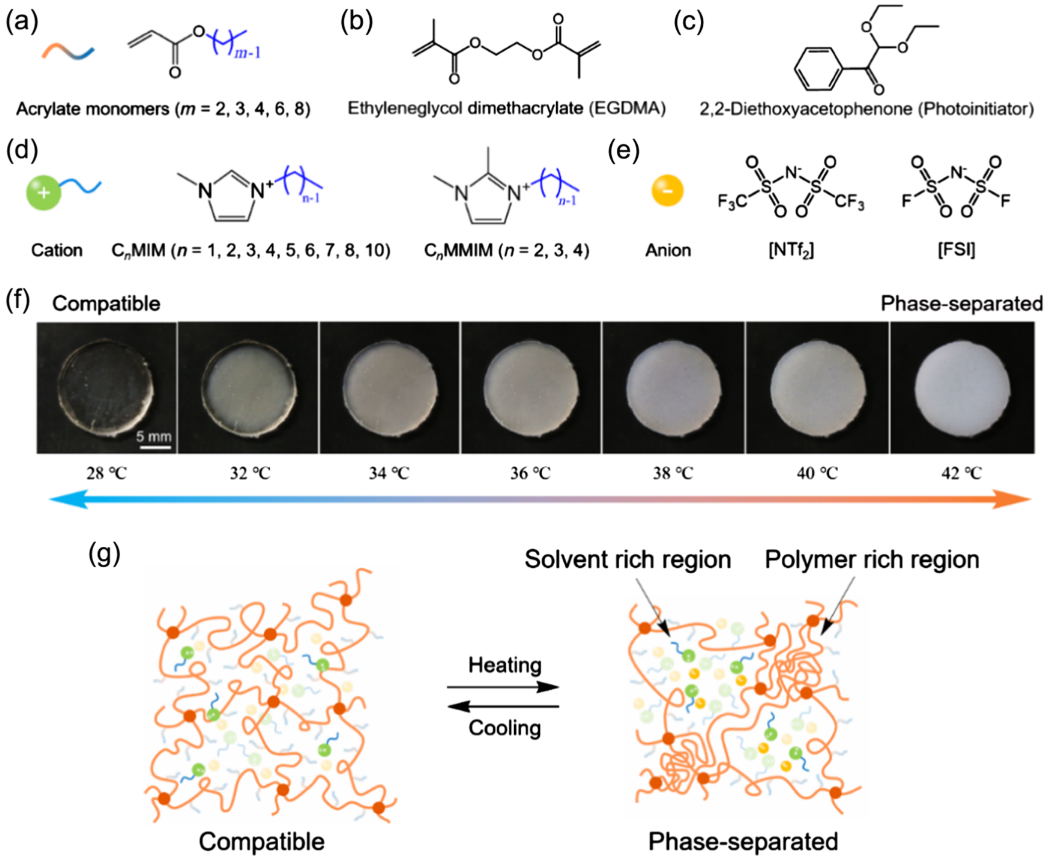

Figure 1 | *Design and fabrication of polyacrylates/[C_nMIM][NTf_2] ionogels. (a) Acrylate monomers with different alkyl chain lengths are utilized to construct the backbone of ionogels. (b) Cross-linker and (c) photoinitiator used in this work. (d) Imidazolium cations with different alkyl chain length and (e) their counter ions. (f) A series of snapshots show the LCST phase behavior of PBA/[C_2MIM][NTf_2] ionogels (2 mm in thickness). (g) Schematic illustration shows the mechanism of LCST phase behavior of PBA/[C_nMIM][NTf_2] systems.*

mechanical resistance and adhesion. The structural formula of acrylate monomers with different alkyl chain lengths is given in Figure 1a. Figures 1d and 1e show the structures of ILs used in this work. The basic physicochemical properties of poly(butyl acrylate) (PBA) ionogels are characterized and given in Supporting Information Figure S2. It is worth noting that different from previous reports stating that [C_2MIM][NTf_2] cannot form transparent and soft ionogels with PBA due to differences in polarity,[35] the as-prepared PBA/[C_2MIM][NTf_2] ionogels are transparent substances without any leakage of ILs at room temperature. We supposed that the PBA/[C_2MIM][NTf_2] ionogel exhibits a LCST phase behavior. This hypothesis is subsequently demonstrated by a thermal response test of the PBA/[C_2MIM][NTf_2] ionogels. As shown in Figure 1f, the transparent PBA/[C_2MIM][NTf_2] ionogel disc quickly becomes opaque as the temperature is increased from room temperature (~25 °C) to 42 °C . Besides, this thermoresponsive phenomenon of the ionogel is completely reversible. Note that no obvious ILs are leaked from the ionogel during this process, and the volume of ionogel remains unchanged at the macroscale before and after phase separation. As a result, the PBA/[C_2MIM][NTf_2] ionogel undergoes rapid, isochoric, and reversible thermoresponsive phase behavior, which is known as LCST phase behavior.

The LCST-type phase separation is a kind of phenomenon where the mixing Gibbs free energy (ΔG_{mix}) changes from negative to positive with increasing temperature. According to the pioneering work by Lee and Lodge,[28] it is believed that the coexistence of structure-forming solvatophobic and solvatophilic groups in the polymer is necessary for LCST phase behavior. Similarly, in PBA/[C_2MIM][NTf_2] ionogel system, the solvatophilic acrylate groups and the solvatophobic *n*-butyl side chains play important roles in the LCST phase behavior of ionogel (Figure 2a). We speculate that the oriented solvation between the polymers and ILs caused by hydrogen-bonding effects and van der Waals interactions may serve as the driving force for the LCST phase behavior in our system. Since hydrogen-bond interaction is stronger than van der Waals interaction, we supposed that the hydrogen bonds serve as the key factor for the LCST phase behavior in this system, which will be discussed later in this work. The van der Waals interaction

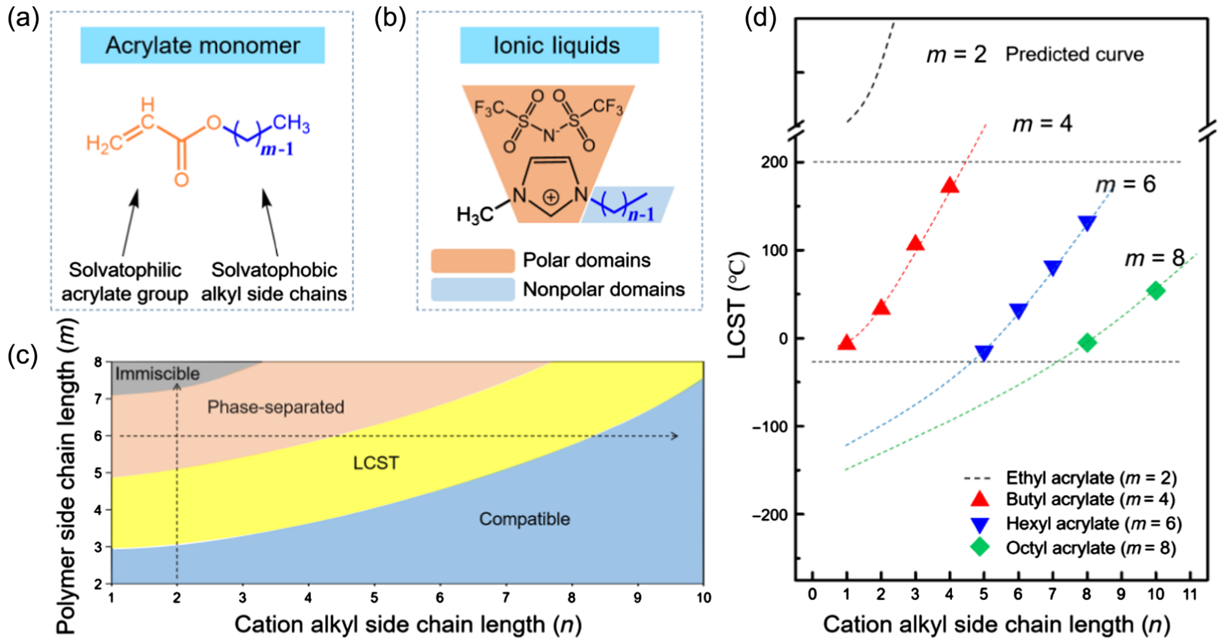

Figure 2 | *Mechanistic analysis and phase diagram of the compatibility of ionogels. (a) Molecular structure and polarity distribution of acrylate monomer. Solvatophilic acrylate (polar) group and solvatophobic alkyl chain (nonpolar) of the acrylate monomer. (b) Molecular structure and polarity distribution of ILs. Polar and nonpolar domains in ILs formed by Coulombic interactions. (c) Phase diagram shows the compatibility of ionogels with different acrylate monomers and ILs. (d) LCST of ionogels as a function of the alkyl chain length on cation.* Compatible: *the as-prepared ionogels were homogeneous and transparent in the temperature range from −20 to 180 °C. It is worth noting that these ionogels also show LCST phase behavior, while the LCST is difficult to detect due to the lower limit of temperature control of the instrument (Supporting Information Figure S3).* Phase-separated: *the acrylate monomers and ILs were miscible, while the as-prepared ionogels were opaque in the temperature range from −20 to 180 °C.* Immiscible: *the acrylate monomers and ILs were immiscible.*

here refers to the interactions between the polar domain of ILs and polar acrylate groups of the polymer backbone, as well as the interaction between nonpolar alkyl substituents on cation of ILs and the nonpolar alkyl side chain on polyacrylates network. The formation of polar and nonpolar domains in ILs is ascribed to Coulombic interactions[36] because the charged groups selectively solvate the charged groups and the uncharged groups (alkyl side chain of imidazolium cations) are expelled from this region as shown in Figure 2b. Herein, $[C_2MIM][NTf_2]$ is a polar domain-dominated IL due to the short side chain on the imidazolium cation. Consequently, for the PBA/$[C_2MIM][NTf_2]$ ionogel at a temperature below its LCST, it was supposed that ILs selectively solvate the solvatophilic acrylate groups close to the polymer backbone, which results in the formation of a homogeneous and transparent ionogel, as shown in Figure 1g (left). The kinetics of thermoresponsive phase separation of ionogels with increasing temperature is described as follows. The hydrogen-bonds and van der Waals interactions between polymer networks and ILs are gradually weakened by heating. When the electrostatic interactions between ILs overwhelm the hydrogen-bonds and van der Waals interactions between polymer networks and ILs, the macroscopic phase separation occurs in the ionogel as shown in Figure 1g (right).

To fundamentally understand the mechanisms of this phase behavior, the effects of structures of polymer and ILs on the LCST of ionogels are systematically investigated (Supporting Information Table S2). The phase diagram in Figure 2c shows the compatibility of ionogels composed of different acrylate monomers and ILs. It is found that the as-prepared ionogels are compatible when the length of the alkyl side chain on polyacrylates is less than three, which is ascribed to the poor solvatophobic effect of the nonpolar domain (short side chain length) on the polymer exerting on the ILs. For certain ILs, miscibility between polymer networks and ILs in ionogels decreased with increasing *n*-alkyl side chain length (nonpolar domain) in polymer networks (n = 2, as indicated by the vertical dotted line in Figure 2c), which is due to the enhanced solvatophobic effect of the nonpolar *n*-alkyl side chain of the polymer on the polar ionic group of ILs. Meanwhile, the miscibility between the polymer network and ILs increased as the alkyl chain length increased on the imidazolium cations of ILs (m = 6, as indicated by the horizontal dotted line in Figure 2c), which is due to the increased affinity between nonpolar components in the polymer (*n*-alkyl side chain) and ILs (alkyl side chain on imidazolium cation) through solvophobic interactions enhancing the ionogel compatibility. To provide a more accurate description of the relationship between molecular structure and phase separation temperature in the current system, the specific phase separation temperature of ionogels in Figure 2c is also summarized and plotted, as shown in Figure 2d. Finally, the prerequisites for the LCST phase behavior of these ionogels are proposed as follows:

1. The coexistence of solvatophobic and solvatophilic groups in the polymer network, corresponding to $n \geq 3$ (alkyl chain length of acrylate) in our system.
2. Matching between the nonpolar domains (m and n) in polymer network and ILs.

Theoretical analysis and molecular dynamics simulation

One empirical interpretation of the LCST phase behavior is based on Flory–Huggins theory. The effective interaction parameter ($\chi_{\rm eff}$) is assumed to follow the functional form:

$$\chi_{\rm eff} = \frac{\alpha}{T} + \beta = \chi_{\rm h} + \chi_{\rm s}$$

The effective interaction can be split into two parts: The first one is the enthalpic part $\chi_{\rm h} = \alpha/T$ with a negative α characterizing the specific attractive interaction due to the hydrogen bonding and the second one is the entropic part $\chi_{\rm s} = \beta$ related to the details of molecular packing. The phase separation occurs when the effective interaction parameter becomes larger than a critical value ($\chi_{\rm eff} = \chi_{\rm c} > 0$), leading to the phase separation temperature:

$$T_{\rm c} = \frac{|\alpha|}{\beta - \chi_{\rm c}}$$

Here, both the numerator and the denominator are positive. When $T < T_{\rm c}$, $\chi_{\rm eff} < \chi_{\rm c}$, the system is homogeneous. When $T > T_{\rm c}$, $\chi_{\rm eff} > \chi_{\rm c}$, the system becomes phase separated. When the cation's alkyl side chain length (n) is increased, this does not affect the hydrogen bonding (α remains almost the same) because the cation has more freedom to adjust its orientation, but the entropic part is reduced because the cation becomes bulky. This leads to a higher value of the LCST temperature $T_{\rm c}$. The trend is different when the acrylate's alkyl side chain length (m) is increased. The solvatophobicity of the long alkyl side chain may contribute to the weakening of the hydrogen bonding (the value of $|\alpha|$ is reduced). Meanwhile, since the acrylate is fixed in a network, the change in the entropic part is small. This leads to a lower value of the LCST temperature $T_{\rm c}$.

The LCST phase behavior of ionogels can also be qualitatively proved by molecular dynamics (MD) simulation. We perform the MD simulation using the large-scale atomic/molecular massively parallel simulator (LAMMPS) to explore the LCST phase transition of the ionogel. In our simulation, we coarse-grain the polymers and cations of ILs as a sequence of connected beads, and model the anions and the cross-linkers as dispersed beads; please see Figure 3a for the schematic illustration of the model and Supporting Information for the simulation details. Our

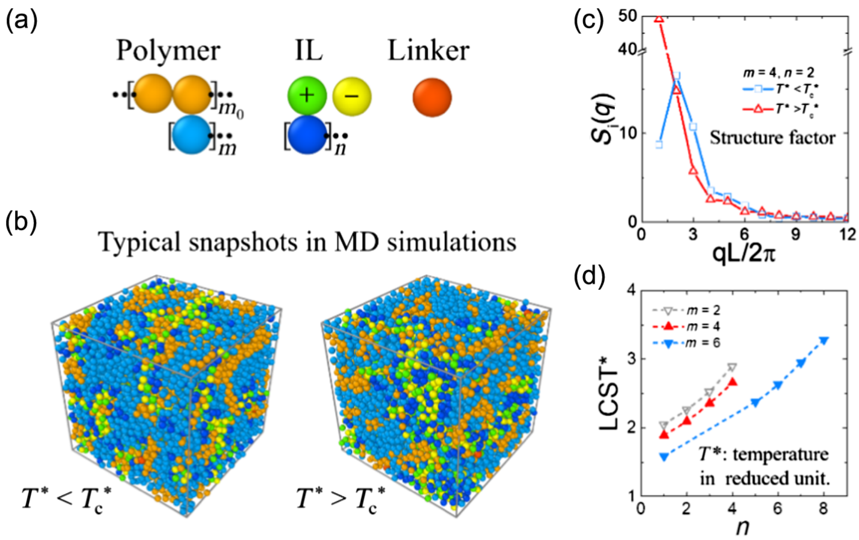

Figure 3 | *MD simulation of the LCST phase separation of the ionogel. (a) Schematics of the coarse-grained polymer, IL, and cross-linker. The orange and light-blue beads represent the solvatophilic backbone and solvatophobic side-chains of the polymers, respectively. The green, dark-blue, and yellow beads represent the headgroup of cations, grafted chain of cations, and anions in the ILs, respectively. (b) Typical simulation snapshots of the ionogel at temperatures below and above the critical temperature* T_c** for LCST phase transition. (c) Structural factor of ionic species* $S_i(q)$*, in which the surge in* $S_i(q)$ *at* $q \sim 0$ *indicates the macroscopic phase separation. (d) LCST of the ionogel at different polymer side-chain lengths and cation chain lengths (T*: temperature in reduced unit).*

simulation indicates that at $T^* = 1.0$, the polymer/ILs mixtures form homogeneous ionogels, in which the ionic species enrich the solvatophilic polymer backbone regions. With increasing temperature, the ionic gelation networks collapse and ILs aggregate, which results in macroscopic phase separation, as shown in Figure 3b. We further estimate the phase transitions of the ionogel by analyzing $S_i(q)$ (Figure 3c) and show the calculated LCST* in Figure 3d. Our simulation illustrates that the variations in cation chain length (n) and polymer side chain length (m) can sensitively affect the LCST of ionogels, as shown in Figure 3d, which is consistent with the experimental data.

The influence of H-bonds on the LCST of ionogels

It is worth noting that H-bonds typically exist in polymer/ILs mixtures, which serves as a dominant factor that results in the LCST phase behavior, as reported by the previous study on PEO/[C_nMIM][BF_4] and polyethers/[C_nMIM][NTf_2] systems.[30-32,37] In addition, in the protein folding process, even if the H-bonds do not directly result in the molecular self-assembly, it can drastically affect the nanostructure of the assembly.[38] Therefore, the effects of hydrogen bonds on LCST phase behavior of ionogel system require further clarification.

Possible hydrogen bonds formed between ILs and polymer backbones in homogeneous PBA/[C_2MIM][NTf_2] ionogels are illustrated as shown in Figure 4a according to the previous studies.[8] As the hydrogen bonds formed between $C_{4,5}$–H of the imidazolium rings and polymer (O atoms of polyacrylate) are much weaker than those via C_2–H, as suggested by Wang and Voth,[39] we have chosen to study hydrogen bonding between C_2–H of imidazolium cation and how the O atoms of PBA influence the LCST of the corresponding ionogel by a controlling variable method. 1-alkyl-2,3-dimethylimidazolium [C_nMMIM][NTf_2] is structurally similar to [C_nMIM][NTf_2], except that a methyl group replaces the H atom in the C_2 position of the ring, as shown in Figure 4b (left). We performed the LCST measurements on the PBA/[C_nMMIM][NTf_2] ionogels. The results are summarized (Supporting Information Table S3) and shown in Figure 4c. It is found that this change (H → CH_3) in ILs structure has a significant influence on the LCST phase behavior of ionogels. For PBA ionogels (60 wt % polymer content), there is a pronounced reduction of about 100 °C in the LCST. Replacing the most acidic proton (C_2) of the imidazolium ring with a methyl group lowers its hydrogen bond-forming capability with the PBA side chain. As a result, without this strong interaction, the miscibility between ILs and PBA is weakened, which causes a decrease in LCST. Besides, the influence of hydrogen bonds between F atoms of the anion and the polymer are also investigated by replacing the CF_3 group with a F atom (Figure 4b, right). The LCST of PBA/[C_nMMIM](fluorosulfonyl)imide[FSI] ionogels is measured and plotted, as shown in Figure 4d. We found

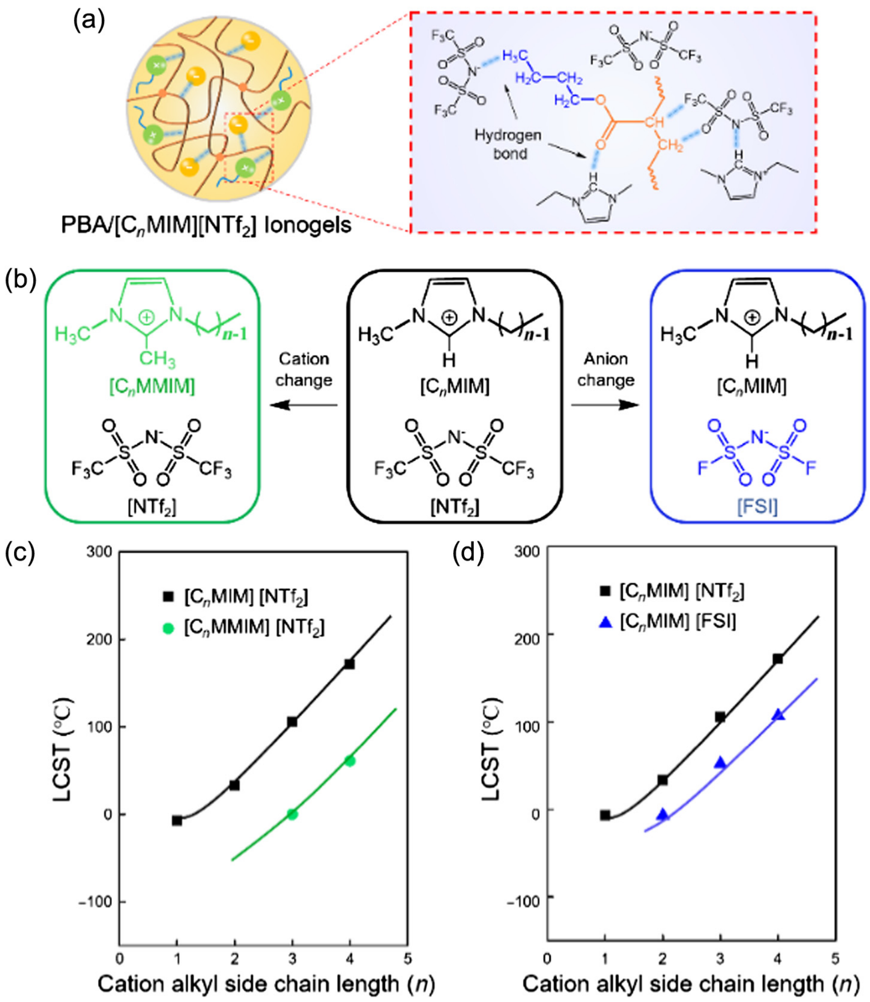

Figure 4 | *Influence of hydrogen bonding on the LCST of PBA ionogels. (a) Schematic illustration shows the hydrogen bonds between ILs and PBA network. (b) ILs with different cations and anions are used to prepare PBA ionogels. (c) The influence of cation type on the LCST of PBA ionogels. (d) The influence of anion type on the LCST of PBA ionogels.*

that the change in the anionic structure of ILs also exhibited a significant influence on the LCST of ionogel. Replacing the CF_3 on anion of ILs with an F atom reduces the number of hydrogen bonds that form between anions with the PBA network, resulting in a reduction of about 60 °C in the LCST of ionogels. These results suggest that the hydrogen bonds between ILs and polymer play an important role in determining the LCST phase behavior of this system.

Continuous regulation of the LCST of ionogels

Further, for certain acrylate monomers, the effects of ILs structure and the content of monomer on the LCST of ionogels are explored. Importantly, we found that a slight increase in alkyl chain length of imidazolium cation results in a huge increase in the LCST of ionogel. As shown in Figure 5a, for PBA ionogels (60 wt % content of monomer), the LCST increased from 32 to 100 °C as the cation's alkyl chain length of ILs increased from 2 to 3. With further increases of the alkyl chain to butyl (4), the LCST of the ionogel reached 175 °C. From a thermodynamic point of view, increasing the alkyl chain length may increase the degree of microphase segregation, which is generated from the polar ionic domains and nonpolar alkyl chain domains.[40-42] The extended microphase segregation in turn lowers the entropy of the ILs, which results in an increase in the LCST of ionogel. Briefly, from the viewpoint of molecular polarity, the extended nonpolar alkyl domains in ILs may enhance the interactions between the ILs and nonpolar domain (butyl side chains and/or alkyl main chain) in PBA, and thus lowers the mixing enthalpy and causes an increase in the LCST. Moreover, it was also found that the LCST of the PBA ionogel increased as the weight fraction of PBA increased from 30 to 60 wt % (Figure 5a). The temperature-composition phase

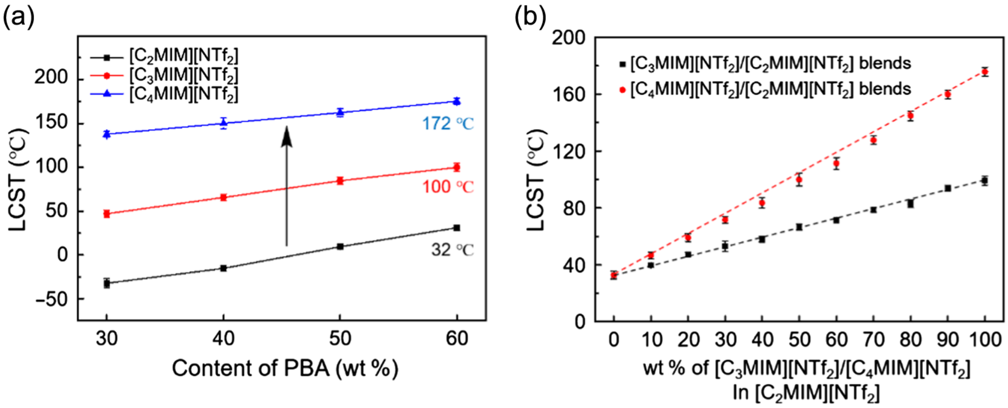

Figure 5 | *Regulating the LCST of PBA ionogels. (a) LCST of PBA ionogels as a function of PBA weight fraction. (b) LCST of PBA (60 wt %) ionogels as a function of the weight fraction of [C_3MIM][NTf_2]/[C_4MIM][NTf_2] in the IL blends.*

diagrams can explain this phenomenon.[28] It is known that the temperature-composition phase diagrams of the LCST system are convex downward. In PBA/ILs systems, the weight fraction of PBA from 30 to 60 wt % may correspond to the rising part of the curve (spinodal curve). Though the polymer/ILs and ionogels are different systems, it could be understood in terms of the results. Furthermore, using IL blends as the solvents, we can regulate the LCST of ionogels almost linearly as the weight fraction of [C_3MIM][NTf_2] and [C_4MIM][NTf_2] increases in the blends, as shown in Figure 5b. These results suggest that the interactions between PBA and ILs do not change significantly upon mixing two structurally similar ILs. Therefore, the IL blends in PBA ionogels are much closer to an ideal random mixing state. Based on this result, continuous regulation of the LCST of ionogels without modifying the chemical structure of the polymers can be realized.

In addition, we found that the LCST of ionogels decreased as the molecular weight of the polymer increased. Such a trend is commonly observed in other polymer/ILs systems that exhibit LCST-type phase behavior,[28,30] as well as our previously reported PBA/ILs system.[34] Consequently, we studied the LCST of PBA ionogels as a function of UV curing time. It was found that the LCST of PBA ionogels first decreased and then reached a plateau with increasing curing time during the preparation of the ionogel (Figure 6a). This may be due to the lower molecular weight of PBA in the ionogel obtained during a short curing time. As a result, the as-prepared PBA ionogels show a relatively high LCST. Taking advantage of this property, reversible thermoresponsive patterned PBA ionogels are fabricated. Schematic illustration in Figure 6b shows the preparation process of patterned ionogels using a photomask with specific patterns. The precursors are placed between two glass slides separated by rubber spacers (1.5 mm in thickness). The solution is first illuminated by UV light (365 nm) for 3 min using a photomask. Then the photomask was removed and the solution was illuminated for another 60 s. Through this strategy, ionogels with graphics, letters, and quick response code patterns were successfully prepared, as shown in Figures 6c–6e, respectively. By alternate heating and cooling, the patterns in the ionogels can be repeatedly displayed.

Finally, taking PBA/[C_2MIM][NTf_2] ionogel as an example, we characterized the thermal stability of ionogel using TGA and DSC. The TGA curve in Supporting Information Figure S5a shows that the ionogels are thermally stable up to 340 °C at 5% weight loss, which suggests that the ionogel exhibited high thermal stability. The glass transition temperatures (T_g) of PBA and PBA ionogel were −47.3 and −60.3 °C , respectively (Supporting Information Figure S5b). The T_g of the PBA ionogel was lower than pure PBA due to the plasticizing effects of the ILs, which is also founded in other ionogel systems.[8,35,43] Besides, the weight of the PBA ionogel remains unchanged even after storing for 30 days in the open air at 25 °C and 50% relative humidity (Supporting Information Figure S6). Consequently, these nonvolatile ionogels with high optical transparency, tunable LCST, good durability, and wide temperature range mechanical stability show promising applications in fields related to flexible sensors and optical devices such as “smart windows”.[44]

Conclusion

In this work, we fabricated a polyacrylates/[C_nMIM][NTf_2] ionogel with LCST-type phase behavior and elucidated the structural effects of ILs and monomers on the LCST phase transition of ionogels. We found that the LCST of ionogels is primarily determined by the polarity of polymer (alkyl) side chains and the alkyl chain on the cation of ILs. The prerequisites for the LCST phase behavior of ionogels are

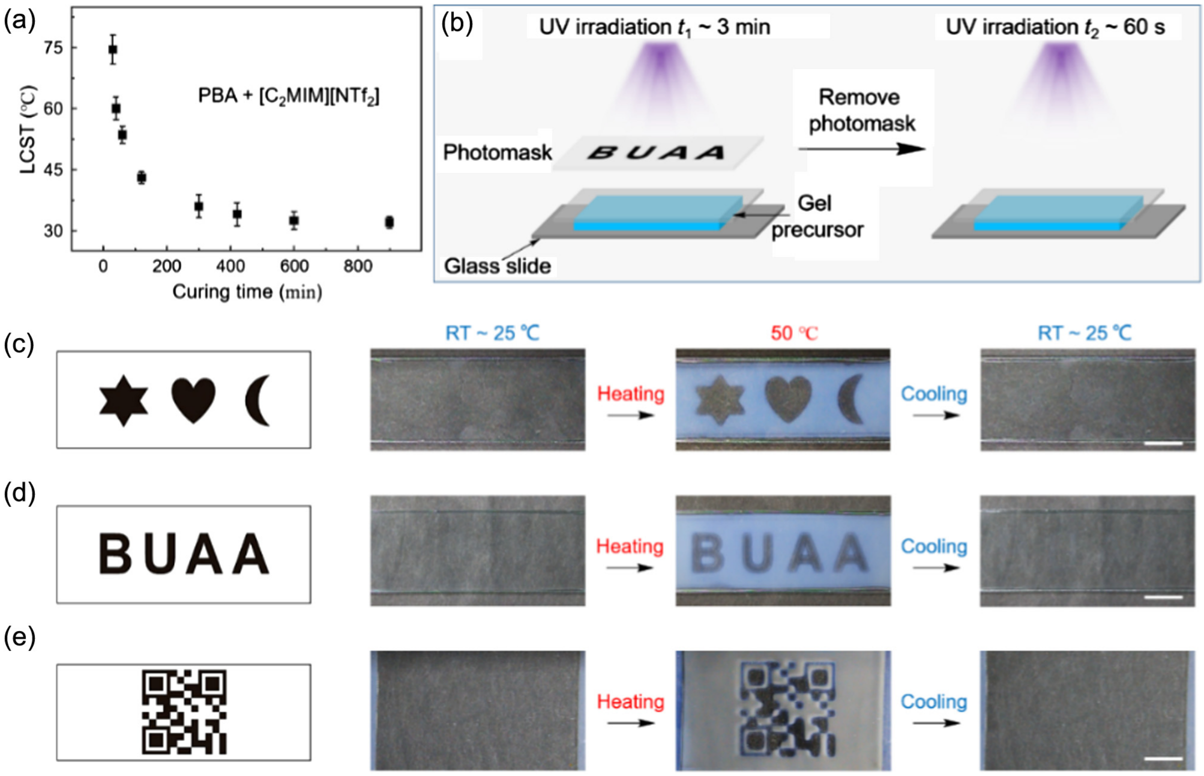

Figure 6 | *Patterning of ionogels. (a) LCST of as-prepared ionogels as a function of curing time (UV irradiation). (b) Schematic illustration shows the preparation of patterned ionogels. Ionogels with graphics (c), letters (d), and quick response code (e) patterns were successfully prepared using photomask. By alternately heating and cooling, the patterns in the ionogels can be displayed repeatedly [scale bars in (c), (d), and (e) were 1 cm].*

proposed as follows: (1) The cosolvatophobic and solvatophilic groups in the polymer network, that is, $n \geq 3$ (alkyl chain length of acrylate) in our system; (2) Matching between the nonpolar domains in the polymer network and ILs. We speculate that the hydrogen-bonding interactions between polymer and ILs are the main driving force for the LCST phase behavior of ionogels, which show significant influence on the LCST of ionogels. In addition, by varying the mixing ratio of two structurally similar ILs in their blends, the LCST of ionogels can be tuned almost linearly through a wide temperature range without modifying the chemical structure of the polymers. Finally, taking advantage of the effects of curing time on the LCST of ionogels, thermoresponsive ionogels with desired patterns are prepared using a photomask. These nonvolatile ionogels with tunable LCST enrich the functionality of current ionogels and provide an alternative to the fabrication of smart flexible electronic and optical devices.

Supporting Information

Supporting information is available and includes the general materials used in this work and a detailed description of the characterization methods. In addition, the mechanical properties, optical properties, and thermal analysis of the ionogels, as well a detailed description of the MD simulation of the ionogels.

Conflict of Interest

There is no conflict of interest to report.

Acknowledgments

This work was financially supported by the National Natural Science Funds for Distinguished Young Scholar (no. 21725401), the National Key R&D Program of China (grant no. 2017YFA0207800), the China Postdoctoral Science Foundation (no. 2019M650434) and the National Natural Scientific Foundation of China (nos. 21774004, 22073094). The authors acknowledge the supports of Computing Center of Jilin Province and Computing Center of CIAC, CAS.

References

1. Rogers, R. D.; Seddon, K. R. Ionic Liquids—Solvents of the Future? *Science* **2003**, *302*, 792–793.
2. Hallett, J. P.; Welton, T. Room-Temperature Ionic Liquids: Solvents for Synthesis and Catalysis. 2. *Chem. Rev.* **2011**, *111*, 3508–3576.

3. MacFarlane, D. R.; Tachikawa, N.; Forsyth, M.; Pringle, J. M.; Howlett, P. C.; Elliott, G. D.; Davis, J. H.; Watanabe, M.; Simon, P.; Angell, C. A. Energy Applications of Ionic Liquids. *Energy Environ. Sci.* **2014**, *7*, 232–250.
4. Le Bideau, J.; Viau, L.; Vioux, A. Ionogels, Ionic Liquid Based Hybrid Materials. *Chem. Soc. Rev.* **2011**, *40*, 907–925.
5. Lodge, T. P.; Ueki, T. Mechanically Tunable, Readily Processable Ion Gels by Self-Assembly of Block Copolymers in Ionic Liquids. *Acc. Chem. Res.* **2016**, *19*, 2107–2114.
6. Osada, I.; de Vries, H.; Scrosati, B.; Passerini, S. Ionic-Liquid-Based Polymer Electrolytes for Battery Applications. *Angew. Chem. Int. Ed.* **2016**, *55*, 500–513.
7. Ding, Y.; Zhang, J. J.; Chang, L.; Zhang, X. Q.; Liu, H. L.; Jiang, L. Preparation of High-Performance Ionogels with Excellent Transparency, Good Mechanical Strength, and High Conductivity. *Adv. Mater.* **2017**, *29*, 7.
8. Cao, Z. Q.; Liu, H. L.; Jiang, L. Transparent, Mechanically Robust, and Ultrastable Ionogels Enabled by Hydrogen Bonding between Elastomers and Ionic Liquids. *Mater. Horiz.* **2020**, *7*, 912–918.
9. Lee, J.; Panzer, M. J.; He, Y. Y.; Lodge, T. P.; Frisbie, C. D. Ion Gel Gated Polymer Thin-Film Transistors. *J. Am. Chem. Soc.* **2007**, *129*, 4532–4533.
10. Cho, J. H.; Lee, J.; Xia, Y.; Kim, B.; He, Y. Y.; Renn, M. J.; Lodge, T. P.; Frisbie, C. D. Printable Ion-Gel Gate Dielectrics for Low-Voltage Polymer Thin-Film Transistors on Plastic. *Nat. Mater.* **2008**, *7*, 900–906.
11. Lee, K. H.; Kang, M. S.; Zhang, S. P.; Gu, Y. Y.; Lodge, T. P.; Frisbie, C. D. "Cut and Stick" Rubbery Ion Gels as High Capacitance Gate Dielectrics. *Adv. Mater.* **2012**, *24*, 4457–4462.
12. Ma, S.; Zhang, Y.; Liang, Y.; Ren, L.; Tian, W.; Ren, L. High-Performance Ionic-Polymer–Metal Composite: Toward Large-Deformation Fast-Response Artificial Muscles. *Adv. Funct. Mater.* **2019**, *30*, 1908508.
13. Tabassian, R.; Nguyen, V. H.; Umrao, S.; Mahato, M.; Kim, J.; Porfiri, M.; Oh, I. K. Graphene Mesh for Self-Sensing Ionic Soft Actuator Inspired from Mechanoreceptors in Human Body. *Adv. Sci.* **2019**, *6*, 10.
14. Trewyn, B. G.; Whitman, C. M.; Lin, V. S. Y. Morphological Control of Room-Temperature Ionic Liquid Templated Mesoporous Silica Nanoparticles for Controlled Release of Antibacterial Agents. *Nano Lett.* **2004**, *4*, 2139–2143.
15. Lunstroot, K.; Driesen, K.; Nockemann, P.; Gorller-Walrand, C.; Binnemans, K.; Bellayer, S.; Le Bideau, J.; Vioux, A. Luminescent Ionogels Based on Europium-Doped Ionic Liquids Confined within Silica-Derived Networks. *Chem. Mater.* **2006**, *18*, 5711–5715.
16. Susan, M. A.; Kaneko, T.; Noda, A.; Watanabe, M. Ion Gels Prepared by in Situ Radical Polymerization of Vinyl Monomers in an Ionic Liquid and Their Characterization as Polymer Electrolytes. *J. Am. Chem. Soc.* **2005**, *127*, 4976–4983.
17. Fukushima, T.; Kosaka, A.; Ishimura, Y.; Yamamoto, T.; Takigawa, T.; Ishii, N.; Aida, T. Molecular Ordering of Organic Molten Salts Triggered by Single-Walled Carbon Nanotubes. *Science* **2003**, *300*, 2072–2074.
18. Fukushima, T.; Asaka, K.; Kosaka, A.; Aida, T. Fully Plastic Actuator through Layer-By-Layer Casting with Ionic-Liquid-Based Bucky Gel. *Angew. Chem. Int. Ed.* **2005**, *44*, 2410–2413.
19. Kamio, E.; Yasui, T.; Iida, Y.; Gong, J. P.; Matsuyama, H. Inorganic/Organic Double-Network Gels Containing Ionic Liquids. *Adv. Mater.* **2017**, *29*, 8.
20. Tang, Z. H.; Lyu, X. L.; Xiao, A. Q.; Shen, Z. H.; Fan, X. H. High-Performance Double-Network Ion Gels with Fast Thermal Healing Capability via Dynamic Covalent Bonds. *Chem. Mater.* **2018**, *30*, 7752–7759.
21. Scott, M. P.; Rahman, M.; Brazel, C. S. Application of Ionic Liquids as Low-Volatility Plasticizers for PMMA. *Eur. Polym. J.* **2003**, *39*, 1947–1953.
22. Ueki, T.; Nakamura, Y.; Usui, R.; Kitazawa, Y.; So, S.; Lodge, T. P.; Watanabe, M. Photoreversible Gelation of a Triblock Copolymer in an Ionic Liquid. *Angew. Chem. Int. Ed.* **2015**, *54*, 3018–3022.
23. Xiong, D. Z.; Cui, G. K.; Wang, J. J.; Wang, H. Y.; Li, Z. Y.; Yao, K. S.; Zhang, S. J. Reversible Hydrophobic-Hydrophilic Transition of Ionic Liquids Driven by Carbon Dioxide. *Angew. Chem. Int. Ed.* **2015**, *54*, 7265–7269.
24. Nguyen, H. H.; El Ezzi, M.; Mingotaud, C.; Destarac, M.; Marty, J. D.; Lauth-de Viguerie, N. Doubly Thermo-Responsive Copolymers in Ionic Liquid. *Soft Matter* **2016**, *12*, 3246–3251.
25. Qiao, Y. X.; Ma, W. B.; Theyssen, N.; Chen, C.; Hou, Z. S. Temperature-Responsive Ionic Liquids: Fundamental Behaviors and Catalytic Applications. *Chem. Rev.* **2017**, *117*, 6881–6928.
26. Ueki, T. Stimuli-Responsive Polymers in Ionic Liquids. *Polym. J.* **2014**, *46*, 646–655.
27. Ueki, T.; Watanabe, M. Lower Critical Solution Temperature Behavior of Linear Polymers in Ionic Liquids and the Corresponding Volume Phase Transition of Polymer Gels. *Langmuir* **2007**, *23*, 988–990.
28. Lee, H. N.; Lodge, T. P. Poly(n-butyl methacrylate) in Ionic Liquids with Tunable Lower Critical Solution Temperatures (LCST). *J. Phys. Chem. B* **2011**, *115*, 1971–1977.
29. Hoarfrost, M. L.; He, Y. P.; Lodge, T. P. Lower Critical Solution Temperature Phase Behavior of Poly(n-butyl methacrylate) in Ionic Liquid Mixtures. *Macromolecules* **2013**, *46*, 9464–9472.
30. Lee, H. N.; Lodge, T. P. Lower Critical Solution Temperature (LCST) Phase Behavior of Poly(ethylene oxide) in Ionic Liquids. *J. Phys. Chem. Lett.* **2010**, *1*, 1962–1966.
31. Kodama, K.; Tsuda, R.; Niitsuma, K.; Tamura, T.; Ueki, T.; Kokubo, H.; Watanabe, M. Structural Effects of Polyethers and Ionic Liquids in Their Binary Mixtures on Lower Critical Solution Temperature Liquid-Liquid Phase Separation. *Polym. J.* **2011**, *43*, 242–248.
32. Lee, H. N.; Newell, N.; Bai, Z. F.; Lodge, T. P. Unusual Lower Critical Solution Temperature Phase Behavior of Poly (ethylene oxide) in Ionic Liquids. *Macromolecules* **2012**, *45*, 3627–3633.
33. Ueki, T.; Watanabe, M. Upper Critical Solution Temperature Behavior of Poly(N-isopropylacrylamide) in an Ionic Liquid and Preparation of Thermo-Sensitive Nonvolatile Gels. *Chem. Lett.* **2006**, *35*, 964–965.
34. Chen, L.; Huang, J.; Zhao, C.; Zhou, J.; Liu, M. Tunable Lower Critical Solution Temperature of Poly(butyl acrylate)

in Ionic Liquid Blends. *Chin. J. Polym. Sci.* **2020**, *39*, 585–591. doi: https://doi.org/10.1007/s10118-021-2522-2

35. Sun, J.; Yuan, Y.; Lu, G.; Li, L.; Zhu, X.; Nie, J. A Transparent, Stretchable, Stable, Self-Adhesive Ionogel-Based Strain Sensor for Human Motion Monitoring. *J. Mater. Chem. C* **2019**, *7*, 11244–11250.

36. Hayes, R.; Warr, G. G.; Atkin, R. Structure and Nanostructure in Ionic Liquids. *Chem. Rev.* **2015**, *115*, 6357–6426.

37. Tsuda, R.; Kodama, K.; Ueki, T.; Kokubo, H.; Imabayashi, S.; Watanabe, M. LCST-Type Liquid-Liquid Phase Separation Behaviour of Poly(ethylene oxide) Derivatives in an Ionic Liquid. *Chem. Commun.* **2008**, *40*, 4939–4941.

38. Baker, E. N.; Hubbard, R. E. Hydrogen Bonding in Globular Proteins. *Prog. Biophys. Mol. Biol.* **1984**, *44*, 97–179.

39. Wang, Z.; Wu, P. Spectral Insights into Gelation Microdynamics of PNIPAM in an Ionic Liquid. *J. Phys. Chem. B* **2011**, *115*, 10604–10614.

40. Wang, Y. T.; Voth, G. A. Unique Spatial Heterogeneity in Ionic Liquids. *J. Am. Chem. Soc.* **2005**, *127*, 12192–12193.

41. Lopes, J. N. C.; Gomes, M. F. C.; Padua, A. A. H. Nonpolar, Polar, and Associating Solutes in Ionic Liquids. *J. Phys. Chem. B* **2006**, *110*, 16816–16818.

42. Russina, O.; Triolo, A. New Experimental Evidence Supporting the Mesoscopic Segregation Model in Room Temperature Ionic Liquids. *Faraday Discuss.* **2012**, *154*, 97–109.

43. Ren, Y. Y.; Guo, J. N.; Liu, Z. Y.; Sun, Z.; Wu, Y. Q.; Liu, L. L.; Yang, F. Ionic Liquid-Based Click-Ionogels. *Sci. Adv.* **2019**, *5*, 10.

44. Ke, Y. J.; Zhou, C. Z.; Zhou, Y.; Wang, S. C.; Chan, S. H.; Long, Y. Emerging Thermal-Responsive Materials and Integrated Techniques Targeting the Energy-Efficient Smart Window Application. *Adv. Funct. Mater.* **2018**, *28*, 18.

Supporting Information for **Finely Tuning the Lower Critical Solution Temperature of Ionogels by Regulating the Polarity of Polymer Networks and Ionic Liquids**

Lie Chen[1,2], Cong Zhao[1], Xiaozheng Duan[3*], Jiajia Zhou[1,4*], Mingjie Liu[1,4*]

[1]Key Laboratory of Bio-Inspired Smart Interfacial Science and Technology of Ministry of Education, School of Chemistry, Beihang University, Beijing, 100191.
[2]School of Physics, Beihang University, Beijing, 100191.
[3]Changchun Institute of Applied Chemistry, Chinese Academy of Sciences, State Key Laboratory of Polymer Physics and Chemistry, Changchun, 130022.
[4]International Research Institute for Multidisciplinary Science, Beihang University, Beijing, 100191.

*Corresponding author: liumj@buaa.edu.cn

Keywords: Ionic liquids, Ionogels, LCST, Polyacrylates, Thermoresponsive, Smart window

1. General materials

All of the following chemical reagents were used as received from Sigma-Aldrich. [Ethyl acrylate (EA), Propyl acrylate (PA), Butyl Acrylate (BA), Tert butyl acrylate (TBA), Hexyl acrylate (HA), Octyl acrylate (OA), Ethyleneglycol dimethacrylate (EGDMA, crosslinker), Diethoxyacetophenone (DEOP, Photo-initiator)]. Ionic liquids were purchased from Lanzhou Yulu Fine Chemical Co., Ltd. [1-Methyl-3-methylimidazolium bis(trifluoromethylsulfonyl)imide ([MMIM][NTf_2]), [EMIM][NTf_2], [PrMIM][NTf_2], [BMIM][NTf_2], [C_5MIM][NTf_2], [C_6MIM][NTf_2], [C_7MIM][NTf_2], [C_8MIM][NTf_2]; [C_2MMIM][NTf_2], [C_3MMIM][NTf_2], [C_4MMIM][NTf_2]; [C_3MIM][FSI], [C_4MIM][FSI]]. The purity of studied ionic liquids was listed below (**Table S1**). Ethanol (AR) and acetone (AR) were supplied by Beijing Chemical Works. Deionized water was obtained via Milli-Q. All photo images in this work were taken by the Cannon 60D.

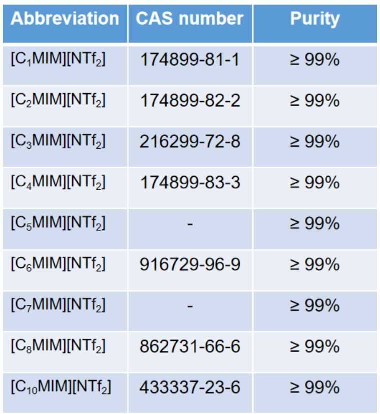

Abbreviation	CAS number	Purity
[C_1MIM][NTf_2]	174899-81-1	≥ 99%
[C_2MIM][NTf_2]	174899-82-2	≥ 99%
[C_3MIM][NTf_2]	216299-72-8	≥ 99%
[C_4MIM][NTf_2]	174899-83-3	≥ 99%
[C_5MIM][NTf_2]	-	≥ 99%
[C_6MIM][NTf_2]	916729-96-9	≥ 99%
[C_7MIM][NTf_2]	-	≥ 99%
[C_8MIM][NTf_2]	862731-66-6	≥ 99%
[C_{10}MIM][NTf_2]	433337-23-6	≥ 99%

Table S1. Purity of ILs used in this work (obtained from http://www.yuluchem.com).

2. Preparation of ionogels

Generally, BA (a sequency of concentration of 30 wt%, 40 wt%, 50 wt%, 60 wt% were prepared), EGDMA (0.2 mol%, 0.5 mol%, 1 mol% of monomer amount) and DEOP (0.1 wt% to monomers) was dissolved in ionic liquid, then the whole mixture was stirred for 10 minutes until fully transparent solution was obtained. The polymerization was initiated by UV irradiation using a mercury arc lamp for 15 min. The resultant hydrogels were rinsed by ample ionic liquid to remove residual monomers.

3. Mechanical characterization

The mechanical characterization of ionogels were realized by using tensile machine (SUNS, UMT4103). The sample were cut into dumbbell shape, 30 mm in length, 5 mm in width, 2 mm in height. Both ends of the dumbbell-shaped sample were connected to the clamps with the lower clamp fixed. The upper clamp was pulled by the load cell at a constant velocity of 20 mm min^{-1} at room temperature, by which the stress–strain curve was recorded and the experimental data was further analyzed. The tensile strength was obtained from the failure point. The modulus was determined by the average slope over 0~10% of strain ratio detected from the stress-strain curve.

The mechanical performance of ionogels were also characterized using Rheometer (Anton Paar, MCR 302). Ionogels with diameter of 1.5 cm and 2 mm thickness were prepared. From -60 □ to 200 □, with a strain of 0.5% and frequency of 1 Hz.

4. Molecular Dynamics Simulation

We categorize the beads as polar (P), apolar (C), and charged (Q) ones [1]. For simplicity, the diameters of all beads are set to be σ. The nonbonded interactions between beads are modeled by the Lennard-Jones (LJ) potential,

$$U_{LJ}(r) = \begin{cases} 4\varepsilon_{LJ}\left[\left(\frac{\sigma}{r}\right)^{12} - \left(\frac{\sigma}{r}\right)^{6} + S\right], r \le r_c \\ 0, r > r_c \end{cases} \quad \text{S(1)}$$

which is shifted to 0 at a cutoff r_c = 1.5 σ by the factor *S*. The interaction parameter ε_{LJ} can assume possible values ranging from weak (1.0) to strong (3.0) to account for the polar, apolar and crosslinking interactions. We use σ = 1.0 (which corresponds to 3 Å) and ε_{LJ}=1.0 (which corresponds $k_B T$ at room temperature) as the length and energy units. The electrostatic interactions between charged beads are described by Coulomb interactions,

$$U_{\mathrm{Coul}} = \frac{Z_1 Z_2 e^2}{4\pi\varepsilon_0\varepsilon_r r} \quad \mathrm{S(2)}$$

where Z_1 and Z_2 represent the valences of the charged species separated in a distance r, e is the elementary charge, ε_0 denotes the vacuum permittivity, and the dielectric constant is set to be ε_r=4 that corresponds to the typical polymer mixtures. We calculate the U_{Coul} using the particle-particle-particle-mesh (PPPM) [2] algorithm with an accuracy of 10^{-5}. The bonded interactions between the connected monomer beads are modeled using the finitely extensible nonlinear elastic (FENE) potential,

$$U_{FENE}(r_b) = -\frac{1}{2}kR_0^2 \ln\left[1-\left(\frac{r_b}{R_0}\right)^2\right] \quad \mathrm{S(3)}$$

where $k = 30\varepsilon_{LJ}^0/\sigma^2$ represents the spring constant and $R_0 = 1.5\ \sigma$ denotes the maximum bond extension. The simulation box contains k = 14 ~ 27 coarse-grained polymer chains. Each polymer consists of $2m_0$ = 100 monomers in the backbone and m = 2, 4 or 6 monomers in the sidechains, and each cation is composed of a positively charged headgroup and a grafted nonchanged chain with its chain length ranging from n = 1 to n = 9. The mole ratios between backbone monomers of the polymers, ILs, and the crosslinkers are set as 100:23:1. We adjust the size of the simulation box to ensure the number density of the bead around 0.86. All simulations are performed in a cubic box with 3D periodic boundary conditions in the canonical (NVT) ensemble using the Large-scale Atomic/Molecular Massively Parallel Simulator (LAMMPS) package [3]. Standard LJ reduced units of the temperature are used in this work and are denoted with a superscript asterisk. Our simulation starts from a random initial configuration. The production runs are firstly performed at T^* = 1.0 for 10^6 MD steps, after which the simulation is conducted over 2×10^6 MD steps by increasing the temperature from T^* = 1.0 to T^* = 3.0. The integration MD time step is 0.004, which corresponds to 5 fs, and the temperature is controlled by the Langevin thermostat.

5. Thermal analysis

The thermal analysis was conducted using a thermogravimetric analyser (TGA) (Q500, TA Instruments, New Castle, DE) and differential scanning calorimeter (DSC)

(Q2000, TA Instruments, New Castle, DE).

6. **LCST characterization of ionogels**

The **LCST** of ionogels were determined by optical transmittance measurements using dynamic light scattering (Anton Paar, Litesizer™ 500). We define the CP values as the temperatures at which the transmittance drops to 80%.

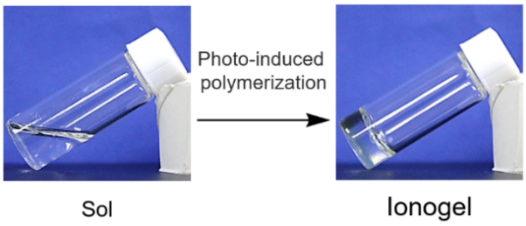

Figure S1. Images show the preparation of poly(butyl acrylate)/[C_2MIM][NTf_2] ionogel by photo-induced polymerization.

Figure S2

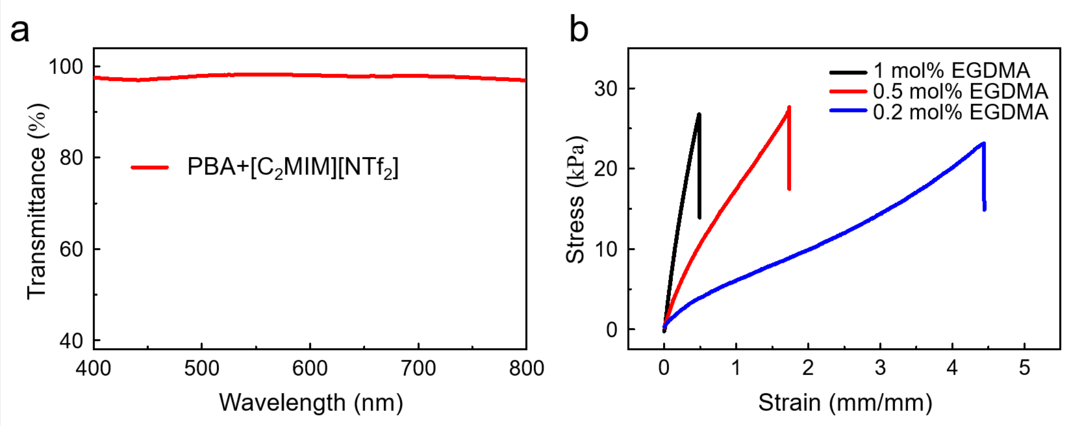

Figure S2. Characterization of the basic properties of PBA ionogels. a) Transmittance of a 0.5 mm thick ionogel in the visible range (400 ~ 800 nm). **b)** Tensile stress–strain curves of ionogels (PBA/[C_2MIM][NTf_2]) with different crosslinking density (weight fraction of PBA is 60%).

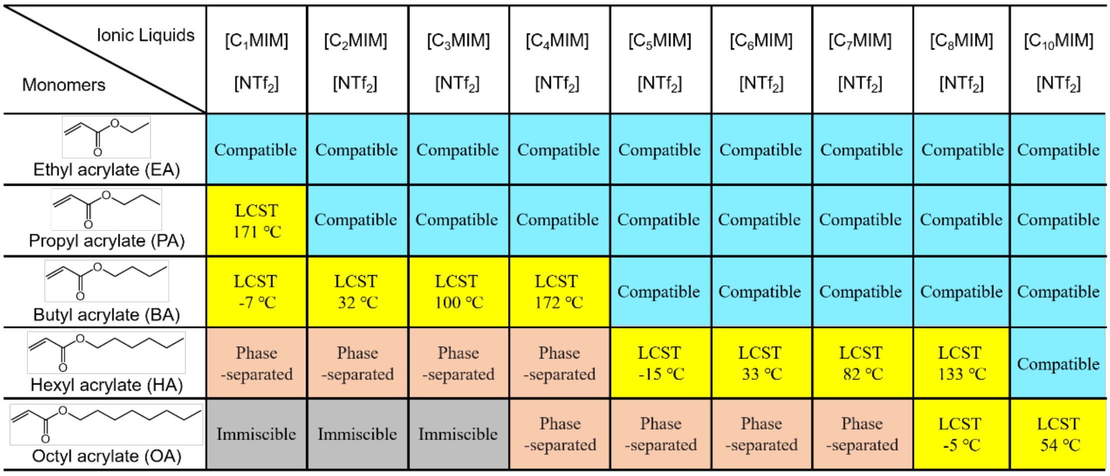

Ionic Liquids Monomers	[C$_1$MIM][NTf$_2$]	[C$_2$MIM][NTf$_2$]	[C$_3$MIM][NTf$_2$]	[C$_4$MIM][NTf$_2$]	[C$_5$MIM][NTf$_2$]	[C$_6$MIM][NTf$_2$]	[C$_7$MIM][NTf$_2$]	[C$_8$MIM][NTf$_2$]	[C$_{10}$MIM][NTf$_2$]
Ethyl acrylate (EA)	Compatible	Compatible	Compatible	Compatible	Compatible	Compatible	Compatible	Compatible	Compatible
Propyl acrylate (PA)	LCST 171 °C	Compatible	Compatible	Compatible	Compatible	Compatible	Compatible	Compatible	Compatible
Butyl acrylate (BA)	LCST -7 °C	LCST 32 °C	LCST 100 °C	LCST 172 °C	Compatible	Compatible	Compatible	Compatible	Compatible
Hexyl acrylate (HA)	Phase -separated	Phase -separated	Phase -separated	Phase -separated	LCST -15 °C	LCST 33 °C	LCST 82 °C	LCST 133 °C	Compatible
Octyl acrylate (OA)	Immiscible	Immiscible	Immiscible	Phase -separated	Phase -separated	Phase -separated	Phase -separated	LCST -5 °C	LCST 54 °C

Table S2. Compatibility of ionogels using different monomers and ionic liquids. Monomers and ionic liquids are mixed at 6 : 4 of weight ratio. Polymerization was carried out in the presence of 1 mol% EGDMA for monomers at RT for 15 min.

Compatible: the as-prepared ionogel was homogeneous and transparent in the temperature range from -20 ~ 180℃.

Phase-separated: the monomer and IL was miscible, the as-prepared ionogel was opaque in the temperature range from -20 ~ 180℃.

Immiscible: the monomer and IL was immiscible.

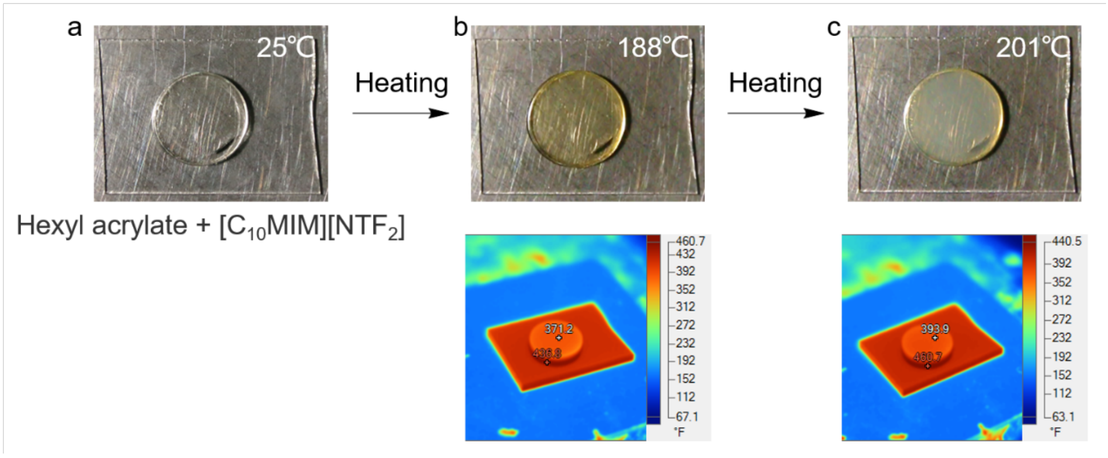

Figure S3. Ionogel with high LCST phase behavior. a) Photograph of ionogel at room temperature. **b)** Photograph of ionogel at high temperature (188□). **c)** Photograph of ionogel when temperature above the LCST (201□).

Ionic Liquids n	[C_nMMIM] [NTf_2]	[C_nMIM] [NTf_2]	[C_nMIM] [FSI]
n = 1		LCST ~ -7 ℃	
n = 2	Phase-separated	LCST ~ 33 ℃	LCST ~ -7 ℃
n = 3	LCST ~ 0 ℃	LCST ~ 106 ℃	LCST ~ 52 ℃
n = 4	LCST ~ 61 ℃	LCST ~ 172 ℃	LCST ~ 107 ℃

Table S3. LCST of PBA ionogels using ionic liquids with different cation side chain length (n) and anions are summarized in table S2.

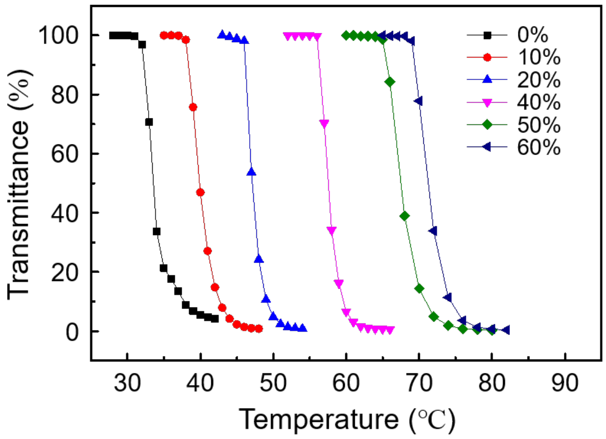

Figure S4. Temperature dependence of transmittance at 658 nm for PBA ionogel measured at a heating rate of ~ 0.5 □/min. Different weight fraction of [C$_3$MIM][NTf$_2$] in ILs blends ([C$_2$MIM][NTf$_2$]/[C$_3$MIM][NTf$_2$]) are investigated.

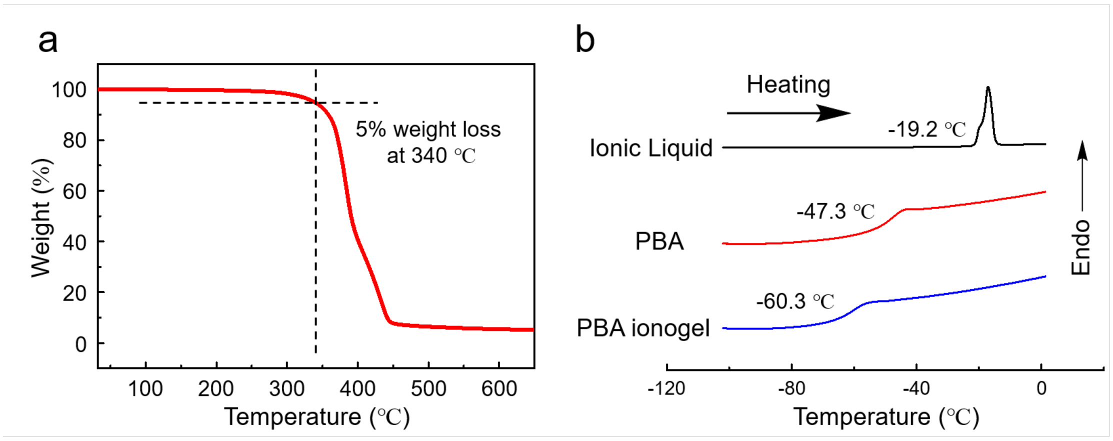

Figure S5. a) TGA curve of PBA/[C_2MIM][NTf_2] ionogel (weight fraction of PBA is 60%). d) DSC curves of the ionic liquid ([C_2MIM][NTf_2]), PBA and corresponding ionogel.

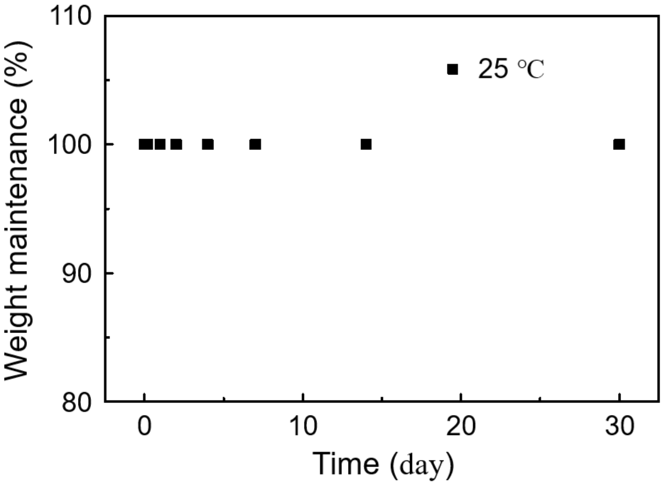

Figure S6. Weight change of the PBA ionogel at 25 □ and 50% relative humidity for 30 days.

Reference

1. Marrink SJ, Risselada HJ, Yefimov S, Peter TD, de Vries AH. The MARTINI Force Field: Coarse Grained Model for Biomolecular Simulations. J Phys Chem B. 2007; 111:7812-24.

2. Darden T, York D, Pedersen L. Particle Mesh Ewald - an N.Log(N) Method for Ewald Sums in Large Systems. Journal of Chemical Physics. 1993; 98(12):10089-92. doi: Doi 10.1063/1.464397. PubMed PMID: ISI: A1993LG10100091.

3. Plimpton S. Fast Parallel Algorithms for Short-Range Molecular-Dynamics. Journal of Computational Physics. 1995; 117(1):1-19. doi: DOI 10.1006/jcph.1995.1039. PubMed PMID: ISI: A1995QK44800001.